Progress In Electromagnetics Research M, Vol. 98, 147–158, 2020

Pattern Reconfigurable Patch Antenna with Dual Band Characteristic for WLAN & 5G Applications

Jinzhi Zhou[1], Ming Yang[1, *], and Junnan Yu[2]

Abstract—A pattern reconfigurable patch antenna with dual band characteristic is investigated in this paper. Two substrates with an air layer of 2 mm is used to design the antenna. Two radiators are respectively printed on the top surfaces of the two substrates. The first radiator, which is the circular patch, is printed on the top surface of the upper substrate. Eight rectangular slots are also introduced to obtain directional radiation pattern with reconfigurable characteristic in low band by changing the current distribution, and no metal layer is printed on the bottom surface of the upper substrate. The second radiator, which is composed of a cross branch and four arc-shaped branches, is printed on the top surface of the lower substrate to provide weak coupling effect with the circular patch. A round ground plane and four symmetrical rectangular slots are printed on the bottom surface of the lower substrate to generate additional resonance point in high band with the characteristic of pattern reconfiguration. A total of 12 PIN diodes are installed in the rectangular slots to verify the accuracy of dual-band and pattern reconfigurable features. The measured result exhibits that the designed antenna has dual band characteristic, in which the low band f_1 is from 2.43 to 2.50 GHz with an average gain of 3.2 dBi and an average radiation efficiency of 73.5%, and the high band f_2 is from 4.83 to 5.03 GHz with an average gain of 5.24 dBi and an average radiation efficiency of 73.9%. Moreover, the measured radiation patterns show that the patterns can be reconfigured at 90-degree intervals simultaneously in two bands.

1. INTRODUCTION

With the increasing demand for broadband and high transmission rate, the high-density user community urges researchers to explore the appropriate method to optimize the wireless environment. Antenna diversity including polarization [1], resonance frequency [2–4], and pattern diversity [5] is utilized as an effective method to mitigate the effect of signal fading caused by multipath scattering [6]. Among them, the diversity of the radiation pattern can be obtained by designing a pattern reconfigurable (PR) antenna. Moreover, the antennas with the characteristic of radiation pattern reconfiguration have received increasing attention from engineers due to the advantages of improved capacity, quality, coverage, and signal propagation efficiency. At present, various methods have been proposed to achieve the characteristic of reconfigurable radiation pattern. In general, these methods can be classified into two types. One is to obtain a modified radiation pattern by changing the structure of the radiator, and the other is to implant PIN diodes on the feeding network to obtain different types of feeding modes. Loading switches on the feedline can also change the resonance frequency. For reference, a quadrilateral patch antenna with frequency agile varying from 2.46 to 3.90 GHz is designed by Kumar and Vijay in [2]. Furthermore, an approach is also employed by incorporating the bias circuit into the ground plane, and not only can the parasitic effects be reduced, but also the performance of the antenna can be improved.

Received 13 August 2020, Accepted 10 November 2020, Scheduled 17 November 2020

* Corresponding author: Ming Yang (myang@ahu.edu.cn).

[1] Electronics and Information Engineering Department, Bozhou University, Bozhou 236800, China. [2] Anhui Sun Create Electronics Co., LTD, Hefei 230000, China.

In [7], a pattern reconfigurable antenna is presented by reconfiguring parasitic strip lines placed around a radiation dipole. The measured result shows that the main beam of the designed antenna can be switched to five specified directions on the elevation plane. In [8], two metal strips composed of PIN diodes and rectangular metallic pixels are placed on the upper surface of the parasitic layer in parallel. After being coupled with the driven patch, an antenna with beam steering and beamwidth variability is designed. Two stacked square patches, a circular patch, and a feeding network with PIN diode are introduced in [9] to design an antenna with the feature of reconfigurable conical and broadside beams. In [10], three orthogonal characteristic modes are obtained by switching the PIN diodes in two feeding networks, then a novel multiple-input multiple-output (MIMO) antenna with reconfigurable pattern is fabricated. Similarly, a broadband reconfigurable feeding network is also proposed in [11] to excite four identical arc dipoles. The experimental results show that the designed antenna can radiate in four different modes with radiation efficiency up to 60%. However, the above-mentioned pattern reconfigurable antennas have a common characteristic, i.e., all antennas only operate in a single band, which limits the multi-scenario application of the antenna. Although it has been proposed in the existing literature [12–15] to achieve diversity patterns and frequency reconfiguration feature based on dual-band antenna, there is very little work to combine the reconfigurable pattern with dual-band antenna. In [16], Yu et al., proposed to etch a rectangular slot on a circular patch to change the current path. Then, an electric dipole is complementary to the magnetic dipole introduced by the turnstile-shaped patch, so that the feature of directional radiation in low band can be realized. However, the measured results show that the antenna can only obtain the pattern reconfigurable characteristics in a single band. In order to solve this problem, we carried out further research on the double-layer patch antenna.

In this paper, an antenna capable of reconfiguring the radiation pattern in two bands is researched and designed. Two stacked circular substrates constitute the overall structure of the dual-band antenna, a circular radiator, and a circular ground plane are printed on the uppermost and lowermost layers of the proposed antenna, respectively. Only one excitation port is introduced for the designed antenna, and the port is directly connected to the turnstile-shaped patch located in the middle layer by center feeding. Compared with [16], a series of rectangular slots are simultaneously etched along a specific position on the circular radiator and ground plane to change the surface current distribution. Moreover, when the proposed antenna resonates at low band and high band, two electric dipoles are introduced. Attributing to the electromagnetic complementary theory, directional radiation can be acquired in two bands. Then, 12 bias circuits are assembled in 12 rectangular slots to electrically switch the state of the rectangular slots. Finally, the radiation pattern of the slotted antenna can be reconstructed in two bands, simultaneously. The measured results show that the antenna has an impedance bandwidth of 2.8% at low band and 4.1% at high band. Moreover, four radiation modes in which the main beams radiated in the directions of $\varphi = 45°$, 135°, 225°, and 315°, respectively, are obtained in both bands by switching the state of the PIN diode.

2. ANTENNA CONFIGURATION AND RECONFIGURABLE PRINCIPLES

The configuration of the proposed PR dual-band antenna is depicted in Fig. 1, and the optimized parameters are also given in Table 1. As shown in Fig. 1, the proposed PR dual-dual-band antenna is composed of substrate 1, an air layer with a height of 2 mm, substrate 2, and an SMA connector from top to bottom. Among them, two Rogers 5880 substrates are selected as substrate 1 and substrate 2, and the only difference is that the thickness of the two substrates are 0.787 mm and 1.575 mm, respectively. In Fig. 1(b), a circular patch is printed on the top surface of substrate 1, and eight rectangular slots are periodically arranged on the circular patch at intervals of 45°. Similarly, it can be seen from Fig. 1(c) that a turnstile-shaped patch and a circular ground plane are printed on the top and bottom surfaces of substrate 2, respectively. It is worth noting that the turnstile-shaped patch is composed of a cross-shaped metal branch and four arcs-shaped branches with a radiance of 64°. At the same time, four rectangular slots are etched along the directions of $\varphi = 45°$, 135°, 225°, 315° on the ground plane for directional radiation in high band.

In order to realize the electrical reconfiguration of the radiation pattern, a total of twelve bias circuits are installed in the rectangular slots. As shown in Fig. 1(b), the bias circuit includes a 47-nH inductance, a 100-pF capacitor, a PIN diode, and two metal pads, similar to [2, 3]. Moreover, the

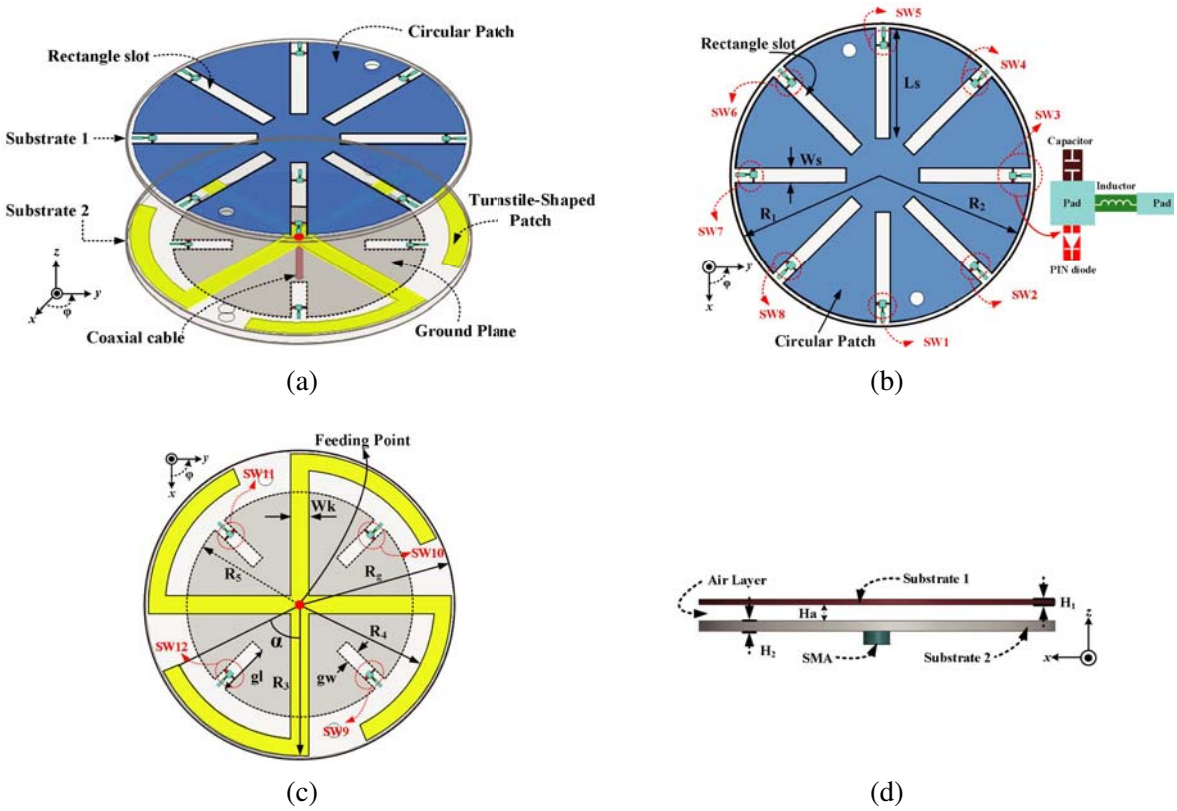

Figure 1. Configuration of the proposed PR dual-band antenna: (a) 3-D view; (b) top view of substrate 1; (c) top view of substrate 2; (d) side view.

Figure 2. Equivalent circuit diagram of PIN diode. (a) ON state; (b) OFF state.

equivalent circuit diagram of the PIN diode is also given in Fig. 2, when the diode is forward biased to realize ON state with 1.5-V DC voltage, and the rectangle slot in which it is placed constitutes a closed state. Conversely, the slot is in the open state, when the diode left unbiased. The bias circuits on the circular patch are arranged in a counterclockwise order from SW1 to SW8, and the bias circuits on the

Table 1. Dimensions of the proposed PR dual-band antenna.

Parameters	on the circular patch				on the turnstile-shaped patch				
	L_s	W_s	R_1	R_2	W_k	R_3	R_4	R_g	α
Values	19.6 mm	2.6 mm	27 mm	26.1 mm	3.2 mm	26.5 mm	23.5 mm	27 mm	64°
Parameters	on the ground plane				The height of two substrates and air layer				
	g_l	g_w	R_5	H_1	H_2			H_a	
Values	9.4 mm	2.4 mm	19.8 mm	0.787 mm	1.575 mm			2 mm	

ground plane also follow the counterclockwise arrangement from SW9 to SW12. It should be noted that the rectangular slots where SW2, SW4, SW6, and SW8 are located correspond to the rectangular slots where SW9, SW10, SW11, and SW12 are located, respectively. These eight rectangular slots are the key point to achieve the simultaneous reconfiguration of the radiation patterns in two bands. Moreover, the proposed PR dual-band antenna is excited by the only one port placed at the center of substrate 2, and a coaxial probe is directly connected to the turnstile-shaped patch. Then, the circular patch is coupling excited, through an air layer with a thickness of 2 mm.

When SW2, 4, 6, 8, 9, 10, 11, 12 are all turned on and the state of the remaining diodes sequentially switched, the radiation modes of the proposed antenna are basically the same as the modes described in [16]. Therefore, these modes will not be discussed in this paper, for brevity. The difference with [16] is that the authors of this paper realized the transition of the high-frequency radiation pattern from omnidirectional to directional by adjusting the position and number of the rectangle slots. In other words, for the antenna designed in this paper, when SW2 and SW9 are in the turn off state and the other switches all turned on, the directional radiation can be obtained at low band and high band.

In order to clearly explain the working principle of the rectangular slots etched on the ground plane and reduce the interference caused by the slots on the circular patch, three simplified antennas are investigated and simulated in Fig. 3. For Ant. 1, from top to bottom are substrate 1, air layer, and substrate 2. A circular patch is printed on the top surface of substrate 1. A turnstile-shaped patch and a ground plane are respectively etched on the top surface and bottom surface of substrate 2. It is worth noting that the three metal layers of Ant. 1 are not loaded with rectangular slots, and the stacked structure is fixed by two nylon screws. Compared with Ant. 1, the improvement made on Ant. 2 is only one rectangular slot located on the circular patch along $\varphi = 45°$. On the whole, Ant. 2 and Ant. 3 have a similar structure, and the only difference is that an additional rectangular slot is added on the ground plane of Ant. 3. Moreover, the longitudinal symmetry axes of the two slots in Ant. 3 must meet the requirement of coincidence on the xoy plane. Three antennas are also analyzed by the commercial electromagnetic simulator software HFSS 15.0 to elaborate the principle of radiation pattern transformation and reconfiguration in high band.

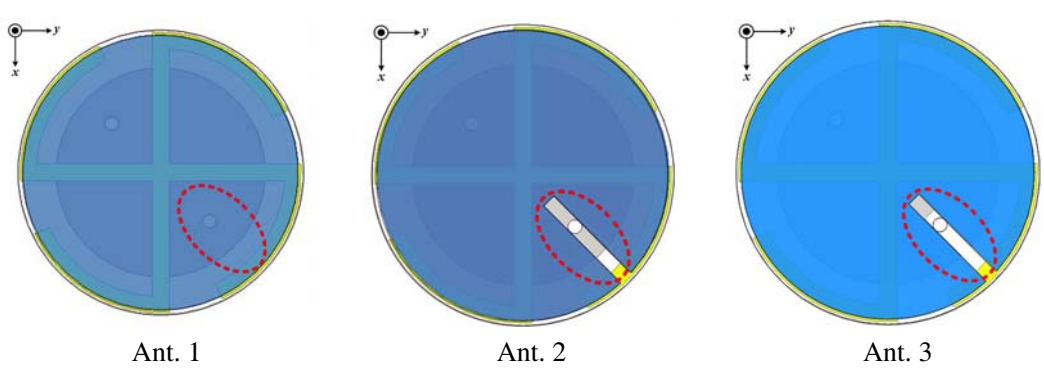

Figure 3. Three forms derived from the evolutionary process of the designed PR dual-band antenna.

As shown in Fig. 4(a), the simulated S-parameter shows that Ant. 1 has two resonance points at 2.45 GHz and 4.90 GHz, but the reflection coefficient amplitude at the two resonance points does not meet the requirement of less than −10 dB. Attributing to the rectangular slots on the circular patch, Ant. 2 has an excellent reflection amplitude at 2.45 GHz, but the rectangular slots have a little tuning effect on impedance matching at high frequencies. Compared with Ant. 2, Ant. 3 has another resonant frequency at 4.90 GHz due to the rectangular slots etched on the ground plane. The simulated results of peak gain are also given in Fig. 4(b). It can be concluded that the gain curve of Ant. 1 is relatively smooth, but the gain amplitude is much smaller than that of Ant. 2 and Ant. 3. Specifically, the simulated gains of Ant. 1 at 2.45 GHz and 4.9 GHz are 2.67 dBi and 4.59 dBi, respectively. On the contrary, the peak gain of the other two antennas at 2.45 GHz are 4.0 dBi with the same fluctuation amplitude. But at 4.90 GHz, the peak gain of Ant. 3 is only 5.5 dBi, which is 0.5 dBi lower than the peak gain of Ant. 2. Combining Fig. 4(a) and Fig. 4(b), it can be obtained that the etched rectangular

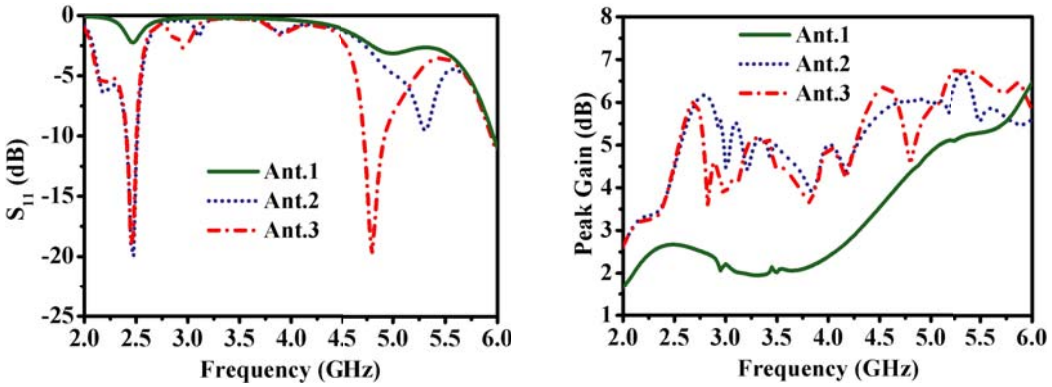

Figure 4. Comparison of the simulated results of three antennas. (a) S_{11}; (b) peak gain.

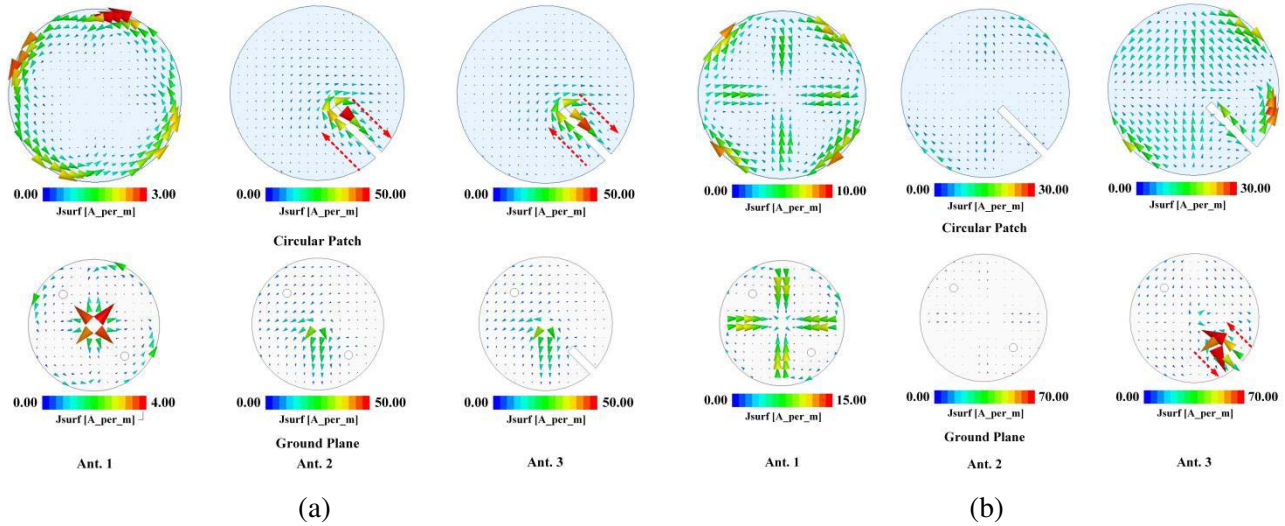

Figure 5. Simulated vector current distributions on the circular patch and ground plane. (a) 2.45 GHz; (b) 4.90 GHz.

slots on the circular patch and ground plane can adjust the impedance matching of Ant. 3 in two bands. Moreover, compared with Ant. 1, the rectangular slots not only change the impedance matching of the antenna, but also improve the gain of the antenna to a certain extent.

In order to vividly explain the resonance principle and radiation mechanism of three antennas, the surface current distributions of three antennas are also given in Fig. 5. From the surface current distribution of Ant. 2 in Fig. 5(a), it can be seen that after the rectangular slots are etched on the circular patch, more current is concentrated on both sides of the rectangular slots, which is in sharp contrast with the current distribution of Ant. 1. Moreover, the length and width of the rectangular slot satisfy Eq. (1), which shows that the rectangular slot has adjusted the impedance matching at 2.45 GHz to a large extent.

$$2L_s + W_s \approx \frac{1}{3}\lambda_l \tag{1}$$

where λ_l represents the wavelength of 2.45 GHz in free space.

For the resonance mode at 4.90 GHz, it can be seen from Fig. 5(b) that more current is concentrated on both sides of the rectangular slots on the ground plane of Ant. 3. Meanwhile, the length and width

of the rectangular slot satisfy Eq. (2).

$$2g_l + g_w \approx \frac{1}{3}\lambda_h \tag{2}$$

where λ_h represents the wavelength of 4.90 GHz in free space. It is worth noting that the rectangular slots in Ant. 2 and the rectangular slots in Ant. 3 play basically the same role, and the only difference is that the rectangular slot functions in a different band.

In order to more intuitively exhibit the transformation of the radiation pattern, the simulated 3-D radiation patterns of the three antennas at 2.45 GHz and 4.90 GHz are given in Fig. 6. Due to the quasi-current loop on the turnstile-shaped patch which similar to that of [16], Ant. 1 exhibits the pattern characteristic of a classical magnetic dipole. In this paper, for the sake of brevity, the surface current distribution on the turnstile-shaped patch is not given. The simulated 3-D radiation pattern of Ant. 2 shows that it is directional radiation at 2.45 GHz and omnidirectional radiation at 4.90 GHz. Among them, the directional radiation is because the rectangular slots etched on the circular patch of Ant. 2 change the current distribution. As shown in Fig. 6(a), more currents concentrated on both sides of the rectangular slot have opposite directions, which causes the energy radiated outward to cancel each other out. Therefore, the working mode of the circular patch behaves as an electric dipole radiating in the direction of $\varphi = 135°$. Then, the electric dipole and magnetic dipole introduced by the turnstile-shaped patch in Ant. 2 satisfy the complementary theory of the magnetoelectric dipole [16], thereby the directional radiation is achieved, shown in Fig. 6(a). However, the rectangular slots on the circular patch have very little disturbance on the current distribution at 4.90 GHz. So Ant. 2 still exhibits omnidirectional radiation at high band. For Ant. 3, slotting on the circular patch and the ground plane at the same time, the consequences can also be seen in Fig. 6(b). When Ant. 3 is excited, two electric dipoles working at 2.45 GHz and 4.90 GHz are introduced respectively. Also benefiting from the complementary theory, two patterns of directional radiation in both bands as shown in Fig. 6(b) are formed. On the other hand, compared with the quasi-omnidirectional pattern of Ant. 2 at 4.90 GHz, Ant. 3 has a directional pattern along the direction of $\varphi = 45°$ at 4.90 GHz.

Through the above theoretical analysis, the rectangular slots etched on the ground plane has a crucial effect on the conversion of the high band radiation pattern, but the effect on the low band is almost negligible. In view of this characteristic, a dual-band pattern reconfigurable antenna is designed in this paper. First, four rectangular slots are etched at $\varphi = 45°$, 135°, 225°, 315° positions of the circular patch to achieve resonance and directional radiation at 2.45 GHz. Meanwhile, four rectangular

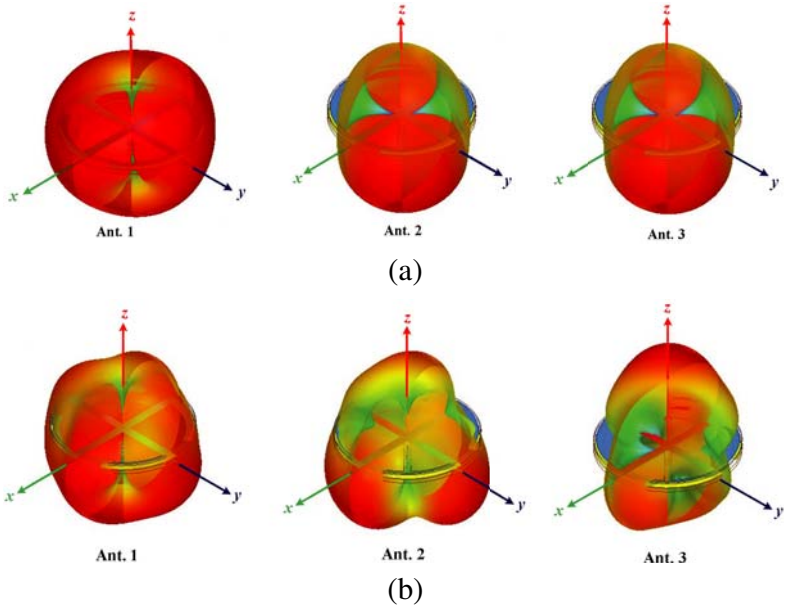

Figure 6. Simulated result of the 3-D radiation pattern. (a) Three antennas at 2.45 GHz; (b) three antennas at 4.90 GHz.

slots are also etched at $\varphi = 45°$, 135°, 225°, 315° positions of the ground plane to achieve resonance and directional radiation at 4.90 GHz. Then, four pairs of PIN diodes are installed in the rectangular slots for electrical reconfiguration of the radiation pattern. In detail, PIN diodes SW2, SW4, SW6, SW8 are installed on the circular patch, and the corresponding PIN diodes SW9, SW10, SW11, SW12 are embedded on the ground plane. Finally, with the four pairs of switches in the off state in sequence and the other switches remaining closed, the proposed antenna has four radiation states in two bands, and the specific states are summarized in Table 2. As shown in Table 2, the main beams of the four states for the two bands radiate along $\varphi = 45°$, $\varphi = 135°$, $\varphi = 225°$, and $\varphi = 315°$, respectively. In order to make the antenna designed in this paper have the characteristics of [16], four additional rectangular slots are etched on the circular patch along the positions of $\varphi = 0°$, 90°, 180°, 270°, and four bias circuits named SW1, SW3, SW5, SW7 are also installed in the above four additional rectangular slots. It is worth noting that only when SW1, SW3, SW5, SW7 are in the off state in sequence and the remaining switches all closed, the antenna exhibits the same characteristics in [16].

Table 2. States of the proposed PR dual-band antenna.

State	SW2 and SW9	SW4 and SW10	SW6 and SW11	SW8 and SW12	SW1 and 3 and 5 and 7	Beam-direction	
I	OFF	ON	ON	ON	ON	f_1 f_2	$\phi = 45°$
II	ON	OFF	ON	ON	ON	f_1 f_2	$\phi = 135°$
III	ON	ON	OFF	ON	ON	f_1 f_2	$\phi = 225°$
IV	ON	ON	ON	OFF	ON	f_1 f_2	$\phi = 315°$

3. DESIGN AND COMPARISON OF THE MEASURED RESULTS

Summarizing the previous analysis, a prototype of the PR dual-band antenna depicted in Fig. 7 is fabricated according to the model in Fig. 1. In order to verify the dual-band and pattern reconfigurable characteristics, an Agilent E5080A network analyzer and an Satimo Starlab near-field measurement system are employed to measure the S-parameter, peak gain, antenna efficiency, and radiation pattern.

Before measuring the S-parameters, for the four groups of switches described above, SW2 and SW9 are off as the first group of switches and the remaining switches are all on. Four sets of tests are conducted in sequence, and the corresponding measured results are shown in Fig. 8. It can be concluded from Fig. 8 that the measured S-parameters of the four states at low band f_1 are lower than -10 dB from 2.43 GHz to 2.50 GHz, which are generally similar to the simulated results. However, compared with the simulated results, the measured resonance frequency of the high band f_2 is shifted. Furthermore, the measured bandwidth ($S_{11} \leq -10$ dB) of f_2 is 200 MHz from 4.83 GHz to 5.03 GHz less than the simulated bandwidth of 430 MHz from 4.85 GHz to 5.28 GHz at f_2. This deviation is caused by the parasitic effect of the bias circuit and the error that occurs during the test.

The measured peak gain and antenna efficiency of the proposed antenna are given in Fig. 9. It is worth to be noted that since the simulated gain and efficiency of the four states are basically the same, only the gain and efficiency of one state are given for brevity. It can be obtained from Fig. 9(a) that the average gain of the four states is 3.2 dBi at f_1, which is lower than the simulated gain of 3.4 dBi. Meanwhile, the measured gain at f_2 is also shown in Fig. 9(a), and the average value of the measured gain in the four states is 5.2 dBi, which is 0.4 dBi lower than the simulated gain.

Figure 7. Prototype of the fabricated PR dual-band antenna. (a) Substrate 1; (b) top surface of Substrate 2; (c) bottom surface of Substrate 2.

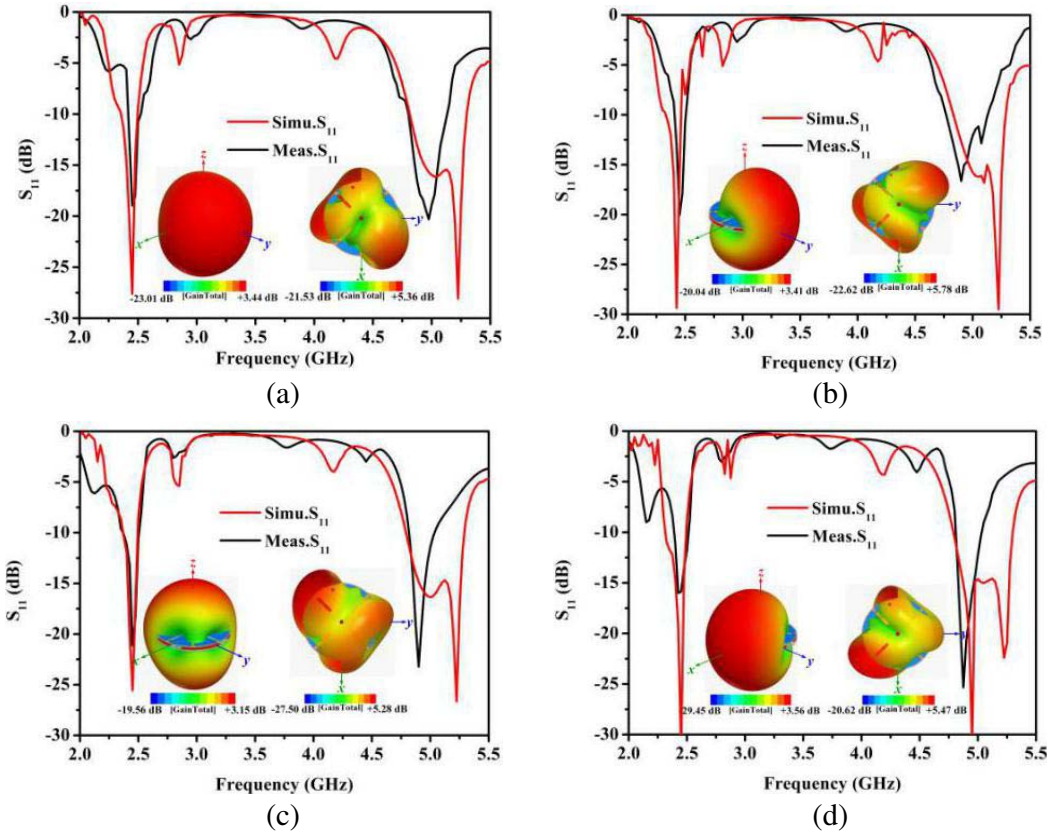

Figure 8. Comparison between simulated and measured results of S-parameters for the four states. (a) State I; (b) State II; (c) State III; (d) State IV.

Figure 9(b) illustrates the simulated and measured efficiencies of the four states. The average values of the measured efficiencies for the four states are 74.8%, 75.1%, 68.8%, and 75.3% at f_1. Compared with the simulated efficiency of 84.3% at f_1, the measured radiation efficiency is lower, which is due to the bias circuit and test error. Similarly, the measured results of the radiation efficiencies at f_2 are 74.1%, 72.9%, 73.7%, and 74.8% lower than the simulated efficiency of 93.2%.

The measured results of the radiation patterns in the four states are also depicted in Fig. 10 and Fig. 11. When the four groups of diodes are switched sequentially in a counterclockwise order, the measured radiation patterns at 2.45 GHz are shown in Fig. 10. It can be concluded from Fig. 10 that the main beam directions of the four state on the yoz-plane are along $\varphi = 45°$, 135°, 225°, 315°, which are consistent with the simulated results. Moreover, for the four states, the measured x-polarization at

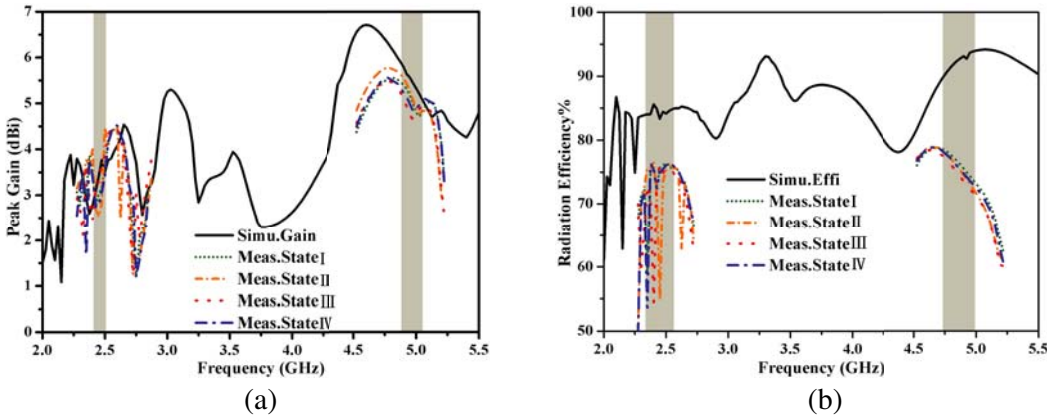

Figure 9. Simulated and measured peak gain and efficiency of the proposed antenna. (a) Peak gain; (b) radiation efficiency.

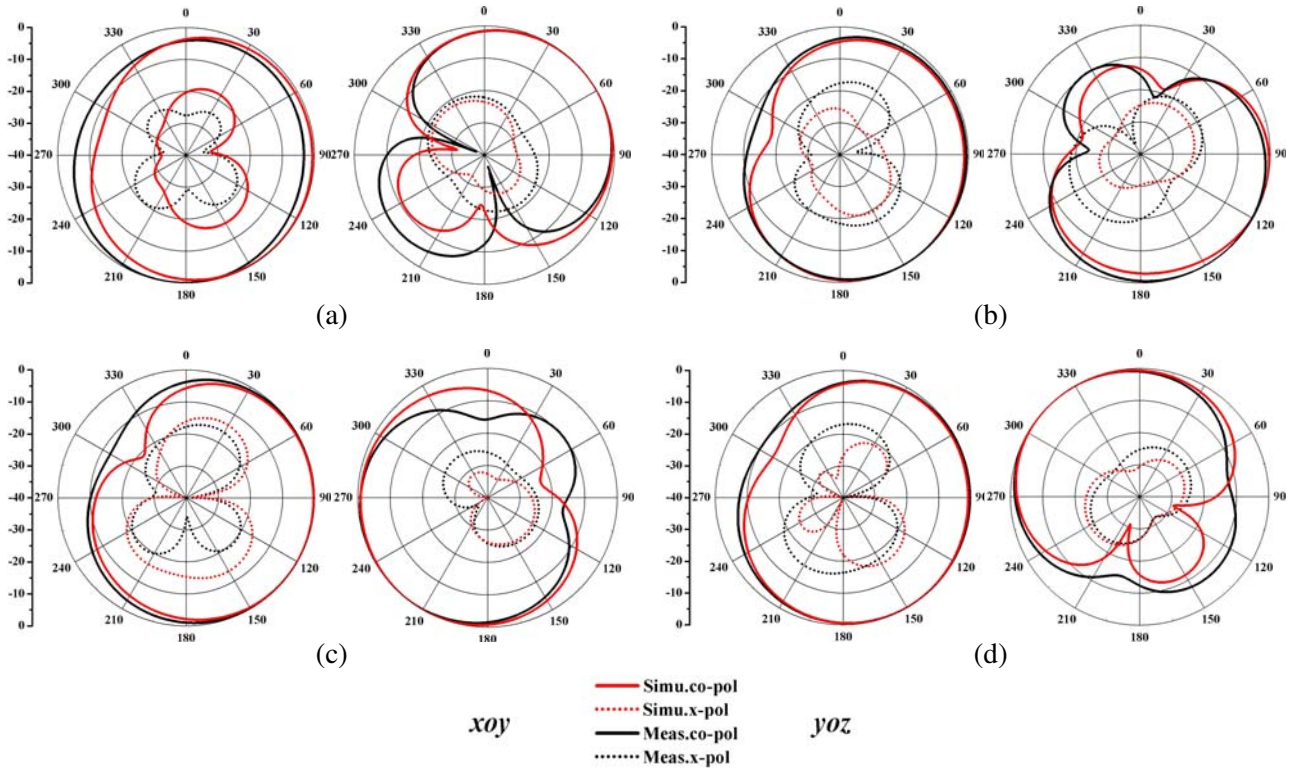

Figure 10. Simulated and measured results of radiation pattern for the PR dual-band antenna in *xoy*-plane and *yoz*-plane at 2.45 GHz. (a) State I; (b) State II; (c) State III; (d) State IV.

the main beam is still −20 dB lower than the co-polarization. Meanwhile, the measured patterns in the *xoy*-plane remains directional radiation with the main beam along the direction of $\varphi = 105°$, as shown in Fig. 10.

When the antenna operates at 4.90 GHz, the corresponding measured results of the radiation pattern are also shown in Fig. 11. Similar to the case of 2.45 GHz, with the switching of the PIN diodes state, the main beam of the directional pattern in the *yoz*-plane radiates successively along the direction of 45°, 135°, 225°, and 315°. At the same time, for the four states, the measured radiation pattern in the *xoy*-plane remains the directional radiation with the main beam direction at 90°.

Some reported antennas are summarized in Table 3 for comparison with the antenna designed in

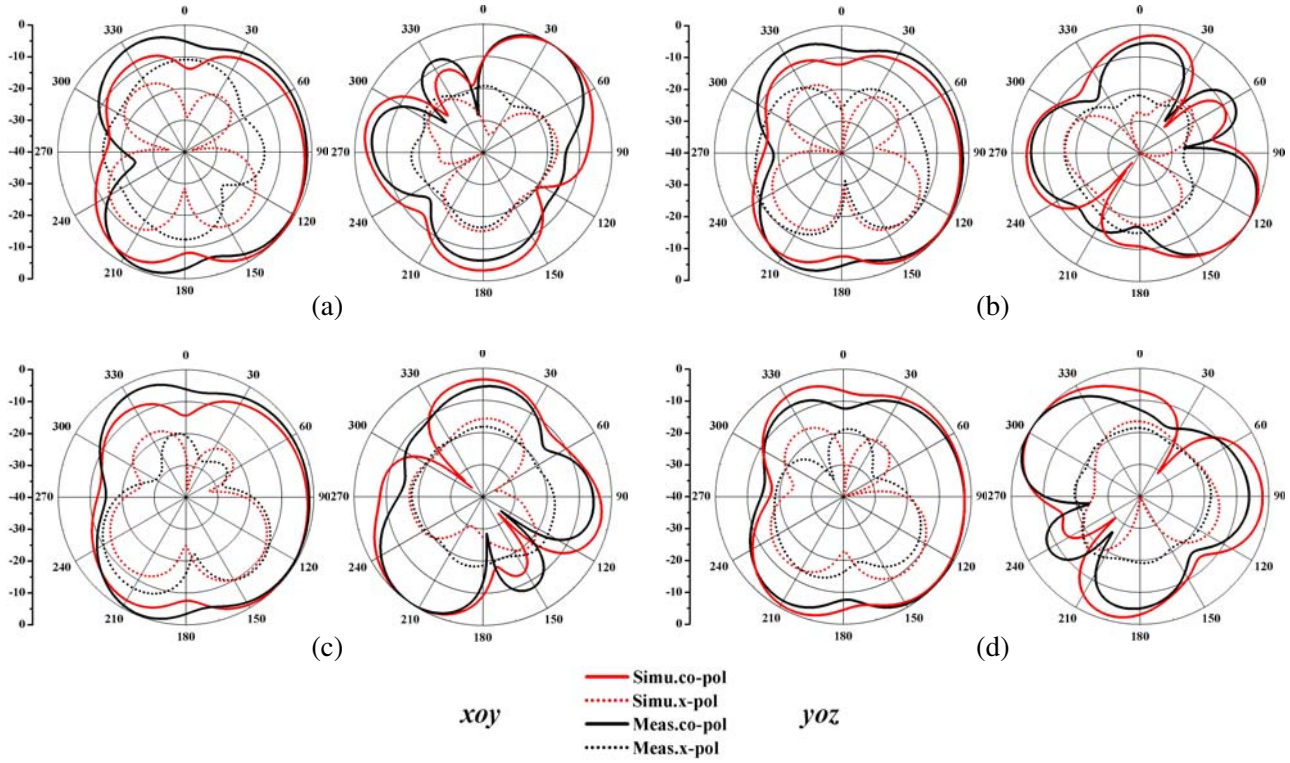

Figure 11. Simulated and measured results of radiation pattern for the PR dual-band antenna in *xoy*-plane and *yoz*-plane at 4.90 GHz. (a) State I; (b) State II; (c) State III; (d) State IV.

Table 3. Comparison between reported and the proposed PR dual-band antenna.

Ref	Impedance Bandwidth (%)	Peak Gain (dBi)	Efficiency (%)	Dual Band	Pattern Reconfigurable	Type	No. of modes	No. of diodes
[7]	-	5.9	> 90	N	Y	No-Planar	5	20
[8]	4	8	> 81	N	Y	Stacked	12	6
[9]	11	2	-	N	Y	Stacked	2	4
[10]	8	-	> 50	N	Y	Planar	3	8
[11]	33.6	4.1	> 60	N	Y	Planar	4	4
[12]	3.39	1.7	> 60	Y	N	Planar	-	0
	9.75	4.5						
[15]	14	4.0	-	Y	N	No-Planar	-	0
	16	4.5						
[16]	2.9	2.9	> 81	Y	N	Stacked	-	4
	2.0	4.8						
[17]	12.2	6	> 80	Y	N	Stacked	-	0
	9.8	7.5						
This work	**2.8**	**3.2**	**> 74**	**Y**	**Y**	**Stacked**	**4**	**12**
	4.1	**5.2**						

this paper. As shown in Table 3, the antennas in [7–11] with different radiation modes are obtained by installing PIN diodes on the radiator or feeding network, but these antennas have only one resonance frequency band, which limits the application range of the antenna. Similarly, in [12, 15–17] some dual-band antennas with high gain, high radiation efficiency, and diversity patterns are presented. However, compared with the pattern reconfigurable antennas, the beam-tunable feature can ensure that the antenna adapts to more complex user distribution scenarios. In this work, the authors combined the dual band and reconfigurable characteristics of the pattern to design an antenna with a frequency ratio up to 2 and four radiation modes, which not only improves the spectrum utilization rate, but also enhances the reliability of the antenna.

4. CONCLUSION

A dual-band patch antenna with the feature of pattern reconfigurability is investigated in this paper. A circular patch etched with eight rectangular slots and a circular ground plane etched with four rectangular slots are located on the top and bottom layers of the antenna, respectively. The introduced rectangular slots change the current distribution on the circular patch and the ground plane, so that the radiation model of the proposed antenna is equivalent to the complementary mode between the magnetic dipole and electric dipole. Finally, attributing to the four rectangle slot (SW2, SW4, SW6, SW8) on the circular patch and the corresponding four rectangular slots (SW9, SW10, SW11, SW12) on the ground plane, the patterns in both bands exhibit directional radiation. Each rectangular slot is equipped with a bias circuit to realize the reconfiguration of the radiation pattern in two bands. The measured results show that the proposed antenna has excellent dual band characteristics. The low band f_1 is from 2.43 GHz to 2.50 GHz with an average gain of 3.2 dBi, and the high band f_2 is from 4.83 GHz to 5.03 GHz with an average gain of 5.2 dBi. With the switching of the specific PIN diodes state, the measured pattern in the yoz-plane shows that the antenna has four radiation modes with low x-polarization and high radiation efficiency in two bands. Based on the dual-band characteristic with a frequency ratio up to 2 and the feature of pattern reconfigurable, the designed antenna can be applied to WLAN and 5G.

5. PROSPECTS FOR FUTURE WORK

With the vigorous development of advanced technology, researchers have gradually begun to use intelligent algorithms to solve problems encountered in practice. For example, Kumar et al. proposed to employ back-propagation network (BPN) to design a hexagonal shaped frequency reconfigurable antenna in [18]. Similarly, an artificial neural network (ANN) model, based on back propagation algorithm, is also proposed for the determination of the resonant frequency of a hexagonal shaped slot antenna in [19]. Borrowing artificial neural networks can help engineers find the most excellent length or height of an antenna by feeding a sufficient number of system training patterns. Furthermore, a trained network allows the reduction of the time needed for the design process of antenna. On the other hand, the ANN not only saves design time but also reduces the complexity of the antenna. The research group plans to utilize artificial neural networks or genetic algorithms to design an antenna that can realize reconfiguration of frequency, polarization and pattern at the same time. Then, an innovative structure will be designed to reduce the number of diodes, and an artificial neural network or an improved genetic algorithm will be introduced to find the most suitable resonance frequency. This not only obtains an antenna with excellent performance in practical applications, but also saves the time and complexity of antenna design.

ACKNOWLEDGMENT

This work was supported by the Key Project of Natural Science Research of Colleges and Universities in Anhui Province under Grant No. KJ2018A0818 and the Scientific Research Project of Bozhou University under Grant No. BYZ2018B01.

REFERENCES

1. Ankit, B., D. Santanu, and K. M. Mrinal, "Polarization-reconfigurable compact monopole antenna with wide effective bandwidth," *IEEE Antennas Wireless Propagation Letters*, Vol. 18, No. 5, 1041–1045, May 2019.
2. Kumar, R. and R. Vijay, "Frequency agile quadrilateral patch and slot based optimal antenna design for cognitive radio system," *International Journal of RF and Microwave Computer-Aided Engineering*, Vol. 28, 1–9, Sep. 2017.
3. Rajeev, K. and V. Ritu, "A frequency agile semicircular slot antenna for cognitive radio system," *International Journal of Microwave Science and Technology*, Vol. 28, 1–9, Apr. 2016.
4. Sanjeev, S. and K. Rajeev, "A frequency re-configurable hexagonal shaped slot antenna for cognitive radio," *International Conference on Next Generation Computing Technologies (NGCT)*, 447–451, Sep. 2015.
5. Yang, X. J., Y. Ji, L. Ge, et al., "A dual-band radiation-differentiated patch antenna for future wireless scenes," *IEEE Antennas Wireless Propagation Letters*, Vol. 19, No. 6, 1007–1011, Apr. 2020.
6. Geng, J., R. Ziolkowski, K. Wang, et al., "Dual CP polarization diversity and space diversity antennas enabled by a compact T-shaped feed structure," *IEEE Access*, Vol. 7, 96284–96296, Jun. 2019.
7. Chen, S., P. Qin, et al., "Pattern reconfigurable antenna with five switchable beams in elevation plane," *IEEE Antennas Wireless Propagation Letters*, Vol. 17, No. 3, 454–457, Mar. 2018.
8. Towfiq, M., I. Bahceci, S. Blanch, et al., "A reconfigurable antenna with beam steering and beamwidth variability for wireless communications," *IEEE Transaction on Antennas and Propagation*, Vol. 66, No. 10, 5052–5063, Oct. 2018.
9. Ding, X., Z. Zhao, Y. Yang, et al., "A low-profile and stacked patch antenna for pattern-reconfigurable applications," *IEEE Transaction on Antennas and Propagation*, Vol. 67, No. 7, 4830–4835, Jul. 2017.
10. Li, K. and Y. Shi, "A pattern reconfigurable MIMO antenna design using characteristic modes," *IEEE Access*, Vol. 6, 43526–43534, Aug. 2018.
11. Jin, G., M. Li, et al., "A simple planar pattern reconfigurable antenna based on arc dipoles," *IEEE Antennas Wireless Propagation Letters*, Vol. 17, No. 9, 1664–1668, Sep. 2018.
12. Sarkar, D., K. Saurav, et al., "Dual band complementary split-ring resonator-loaded printed dipole antenna arrays for pattern diversity multiple-input-multiple-output applications," *IET Microwave & Antennas Propagation*, Vol. 10, No. 7, 1113–1123, Jul. 2016.
13. Ge, L., M. Li, J. Wang, et al., "Unidirectional dual-band stacked patch antenna with independent frequency reconfiguration," *IEEE Antennas Wireless Propagation Letters*, Vol. 6, 113–116, Apr. 2017.
14. Famoriji, O., S. Yang, Y. Li, et al., "Design of a simple circularly polarised dual-frequency reconfigurable microstrip patch antenna array for millimeter-wave applications," *IET Microwave & Antennas Propagation*, Vol. 13, No. 10, 1671–1677, Aug. 2019.
15. Liu, X., Y. Wu, Z. Zhuang, et al., "A dual-band patch antenna for pattern diversity application," *IEEE Access*, Vol. 6, 51986–51993, Sep. 2018.
16. Yu, J., Y. Sun, H. Fang, et al., "A novel stacked patch antenna with dual band and diverse pattern characteristics," *Microwave and Optical Technology Letters*, Vol. 62, No. 1, 1–13, Sep. 2019.
17. Gao, S., L. Ge, D. Zhang, et al., "Low-profile dual-band stacked microstrip monopolar patch antenna for WLAN and car-to-car communications," *IEEE Access*, Vol. 6, 69575–69581, Oct. 2018.
18. Kumar, R., K., P. Kumar, S. Singh, and R. Vijay, "Fast and accurate synthesis of frequency reconfigurable slot antenna using back propagation network," *International Journal of Electronics and Communication*, Vol. 112, 1–10, Dec. 2019.
19. Kumar, R., K., P. Kumar, and R. Vijay, "Hexagonal shaped slot antenna resonant frequency determination using ANN approach," *Microwave Review*, Vol. 25, 27–30, Jun. 2019.